

Superconducting critical fields of single-crystalline $\text{K}_{0.73}\text{Fe}_{1.68}\text{Se}_2$

M. I. Tsindlekht,¹ I. Felner,¹ M. Zhang,² A. F. Wang,² and X. H. Chen²

¹*The Racah Institute of Physics, The Hebrew University of Jerusalem, 91904 Jerusalem, Israel*

²*Hefei National Laboratory for Physical Science at Microscale and Department of Physics, University of Science and Technology of China, Hefei, Anhui 230026, People's Republic of China*

(Received 1 May 2011; revised manuscript received 26 May 2011; published 8 August 2011)

We report the results of an experimental study of dc and low-frequency magnetic properties of a $\text{K}_{0.8}\text{Fe}_{2-y}\text{Se}_2$ single crystal when the dc magnetic field is applied parallel to the **ab** plane. From the data obtained, we deduce the full H - T phase diagram, which consists of all three $H_{c1}(T)$, $H_{c2}(T)$, and $H_{c3}(T)$ critical magnetic-field plots. The two $H_{c1}(T)$ and $H_{c2}(T)$ curves were obtained from dc magnetic measurements, whereas the surface critical-field $H_{c3}(T)$ line was extracted by ac susceptibility studies. It appears that near T_c , the $H_{c3}(T)/H_{c2}(T)$ ratio is ≈ 4.4 , which is much larger than expected.

DOI: [10.1103/PhysRevB.84.052503](https://doi.org/10.1103/PhysRevB.84.052503)

PACS number(s): 74.70.Xa, 74.25.Op, 74.70.Ad

Over the past four decades, the ternary intermetallic compounds, which crystallize in the body-centered tetragonal ThCr_2Si_2 (space group $I4/mmm$), have been of great interest due to the variety of physical phenomena observed in these materials. As early as 1973, both magnetic and Mössbauer (MS) effect spectroscopy studies suggested that in $R\text{Fe}_2M_2$ (R = rare earth; M = Si or Ge), the Fe ions are diamagnetic.¹ Indeed, neutron powder diffraction measurements on NdFe_2Si_2 confirmed the absence of any magnetic moment on the Fe sites, and determined that the Nd sublattice is antiferromagnetically (AFM) ordered at $T_N \approx 16$ K, with the moments aligned along the **c** axis.²

At high temperatures, both BaFe_2As_2 and $M\text{Fe}_2\text{Se}_2$ (M = K, Rb, Cs, Tl/K, and Tl/Rb) pristine materials also crystallize in this tetragonal ThCr_2Si_2 type structure. The common properties of these systems are that the Fe-As and Fe-Se layers exhibit long-range three-dimensional AFM order at $T_N \approx 140$ – 150 and 520 – 550 K, with Fe^{2+} moments of $0.87(3)$ μ_B/Fe or 3.3 μ_B/Fe , respectively. In BaFe_2As_2 , the Fe moments are aligned within the **ab** plane,³ whereas in $M\text{Fe}_2\text{Se}_2$ they are along the **c** axis.⁴ Also associated with or preceding the magnetic transition is a structural transition: tetragonal to orthorhombic for the pnictides, and tetragonal ($I4/mmm$) to another tetragonal ($I4/m$) structure for the Fe-Se based materials. The major difference between the two systems, noticeable from several types of measurements, is that in the Fe-As based materials the temperature composition complex phase diagrams show a generic behavior as a function of the substituent concentration (x). This implies a systematic suppression of the magnetic transition by increasing x by either electrons or holes.⁵ Then, above a critical concentration (which depends on the substituent), superconductivity is observed. Indeed, partial substitution of Ni or Co for Fe in BaFe_2As_2 induces superconductivity (SC) in the $\text{Ba}(\text{Fe}_{1-x}\text{Ni}_x)_2\text{As}_2$ and $\text{Ba}(\text{Fe}_{1-x}\text{Co}_x)_2\text{As}_2$ systems.^{5,6} On the other hand, the nonstoichiometric $M_x\text{Fe}_{2-x}\text{Se}_2$ materials also become superconductive around 30 – 33 K, but the AFM state persists even at low temperatures. That means that in $M_x\text{Fe}_{2-x}\text{Se}_2$ a real coexistence of the two states occurs, since both states are confined to the same Fe-Se crystallographic layer.⁷ This peculiar property marks such a system as a very unique one and opens a new avenue for the study of the interplay between magnetism and superconductivity.

So far, the bulk upper critical magnetic field (H_{c2}) for $\text{M}_x\text{Fe}_{2-x}\text{Se}_2$ single crystals has been determined over a wide range of temperatures and magnetic fields. For $\text{K}_{0.8}\text{Fe}_{1.76}\text{Se}_2$, the field dependence of the resistivity at low dc fields (H_0) and the radio frequency penetration depth in a pulsed magnet up to 60 T exhibit an anisotropy in H_{c2} when measured along or perpendicular to the **c** axis.⁸ Generally speaking, a linear temperature dependence of H_{c2} in both directions is observed and the slope close to T_c is higher for H_0 parallel to the **ab** plane. The initial anisotropy factor γ is ≈ 2 .⁸ Similar results were obtained for $\text{Tl}_{0.58}\text{Rb}_{0.42}\text{Fe}_{1.72}\text{Se}_2$, where the extrapolation to $T = 0$ yields $H_{c2}(0)$ 221 and 44.2 T (an anisotropy $\gamma \approx 5$) for H_0 parallel or perpendicular to the **ab** plane, respectively.^{9,10}

In this work, we report on the temperature dependence of the three critical fields H_{c1} , H_{c2} , and H_{c3} in a $\text{K}_{0.8}\text{Fe}_{2-y}\text{Se}_2$ ($y = 0.25$) single crystal ($T_c \approx 31$ K) measured in a magnetic field applied parallel to the **ab** plane. Both $H_{c1}(T)$ and $H_{c2}(T)$ plots were deduced from dc $M(H_0)$ and $M(T)$ curves. In addition, the $M(H_0)$ curve at 35 K (above T_c) is not linear as expected for an AFM material, but rather exhibits a small peculiar hysteresis loop, which is shifted from the origin, known as the exchange biased field phenomenon. These observations are compared with earlier reports on similar materials. A $H_{c3}(T)$ plot was obtained by ac susceptibility measurements. It appears that, near T_c , $H_{c3}/H_{c2} \approx 4.4$, a value that is much higher than the 1.7 predicted for conventional SC material.¹¹

A single crystal with the nominal composition of $\text{K}_{0.73}\text{Fe}_{1.68}\text{Se}_2$ single crystal was grown in Hefei by the conventional high-temperature flux method.^{7,12} The actual composition of this crystal as determined by various methods is $\text{K}_{0.73}\text{Fe}_{1.68}\text{Se}_2$, as described in Ref. 13. The sizes of the roughly triangular-shaped sample are 7 mm (width), 3 mm (height), and 1.5 mm (thickness). The crystal plate is perpendicular to the **c** lattice axis. The temperature and/or field dependence of the dc magnetic moment was measured in a commercial MPMS5 Quantum Design superconducting quantum interference device (SQUID) magnetometer. Prior to recording the zero-field-cooled (ZFC) curves, the SQUID magnetometer was always adjusted to be in a “real” $H_0 = 0$ state. The ac susceptibility χ' and χ'' was measured with the pickup coil method at amplitude $h_0 = 0.05$ Oe and frequency 1465 Hz. The sample was inserted into one coil of a balanced

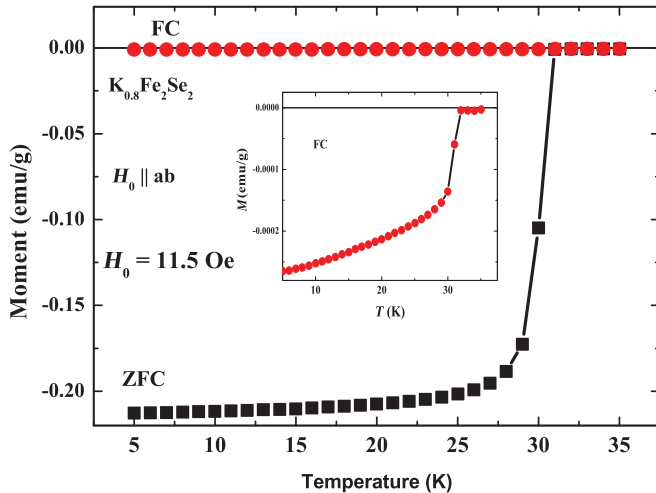


FIG. 1. (Color online) ZFC and FC plots measured at 11.5 Oe. The FC branch in an extended scale is shown in the inset.

pair. The amplitude and phase of the unbalanced signal were measured by a lock-in amplifier in a point-by-point mode. The “homemade” measurement cell of the experimental setup was adapted to the SQUID magnetometer. The block diagram of this setup was published elsewhere.¹⁴ All measurements have been performed for dc and ac fields parallel to the **ab** plane.

(i) *M(T) curves.* The ZFC and field-cooled (FC) magnetization curves of $K_{0.8}Fe_{2-y}Se_2$ were measured at 11.5 Oe and are depicted in Fig. 1. The ZFC branch shows a diamagnetic transition at $T_c = 31.0 \pm 0.5$ K. This transition is not sharp (as expected for a single crystal SC) and it is similar to inhomogeneous materials with a distribution of T_c related to the small spread of stoichiometry inside the sample. The negative FC branch is also shown in the inset. The estimated shielding fraction is about $-1/4\pi$ emu/cc.

(ii) *Isothermal $M(H_0)$ curves.* Isothermal magnetization curves have been measured at various temperatures and selected $M(H_0)$ plots measured at 5, 20, 26, and 29 K are shown in Fig. 2. In the Meissner state, the $M(H_0)$ curves are linear and $H_{c1}(T)$ is defined as the field in which $M(H_0)$ deviates from linearity (Fig. 2, lower inset).¹⁵ Temperature dependence of H_{c1} plotted in Fig. 3 (inset) does not follow the conventional BCS behavior. The extrapolation of this curve to $T = 0$ yields $H_{c1}(0) \approx 130 \pm 10$ Oe. The calculated demagnetization factor for this sample is ≈ 0.1 . Thus the correction to H_{c1} is about 15 Oe at low temperatures.

The criterion for determining the upper critical field $H_{c2}(T)$ requires consistency, and no one method is entirely unambiguous. The $H_{c2}(T)$ values (Fig. 3) were obtained by measuring $M(T)$ dependence under various applied fields and $H_{c2}(T)$ was defined as the onset of the negative signal of the ZFC branches as depicted in Fig. 2, inset. Alternatively, above T_c (at 35 K) for high enough applied fields, the measured $M(H_0)$ plot is a straight line. $H_{c2}(T)$ for the various $M(H_0)$ plots shown in Fig. 2 were determined as the fields in which they deviate from this straight line (marked by an arrow in Fig. 5). The two methods yield practically the same $H_{c2}(T)$ values, presented in Fig. 3. Due to the high T_N of the crystal, it is assumed that the same $M(H_0)$ line in the normal state can be used for extraction of $H_{c2}(T)$, as shown in Fig. 3. By

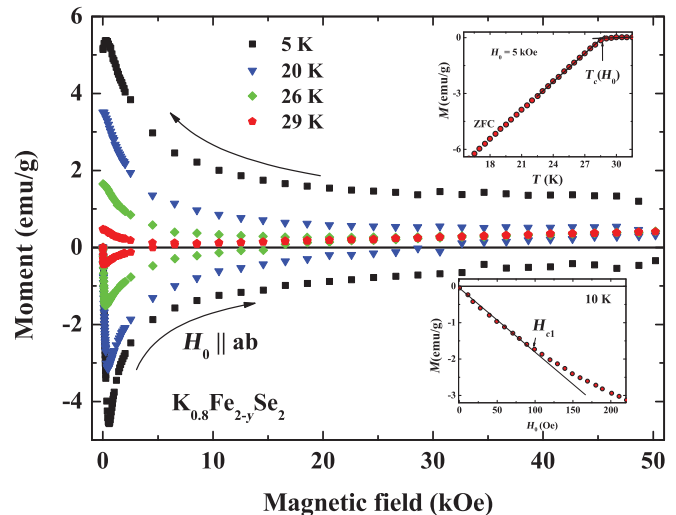


FIG. 2. (Color online) Ascending and descending branches of $M(H_0)$ curves at various temperatures. Lower inset: determination of H_{c1} . Upper inset: determination of H_{c2} .

using the well-known Werthamer-Helfand-Honenberg (WHH) formula:¹⁶ $H_{c2}(0) = -0.69T_c(dH_{c2}/dT)$, where $T_c \approx 31$ K and the linear slope (close to T_c) dH_{c2}/dT is -9 kOe/K, Fig. 3, $H_{c2}(0)$ obtained is 193 ± 6 kOe, a value which is an order of magnitude smaller than that estimated for the same orientation in $Tl_{0.58}Rb_{0.42}Fe_{1.72}Se_2$ ⁷ and $K_{0.8}Fe_{1.8}Se_2$.⁸ It is well accepted that the WHH formula is valid for one-band superconductors and that $H_{c2}(0)$ might be affected by the complicated multiband structure as observed in various Fe-Se crystals.¹⁷ Hence this $H_{c2}(0)$ is just a rough estimation. An accurate value can only be achieved by applying high enough magnetic fields. However, for a similar $K_{0.8}Fe_{1.72}Se_2$ crystal, $H_{c2}(0)$ is well above 60 T as shown in Ref. 8.

Using the Ginzburg-Landau (GL) relation for the coherence length, $\xi = (\Phi_0/2\pi H_{c2})^{1/2}$, we obtained for $K_{0.8}Fe_{2-y}Se_2$ $\xi(0) \approx 10$ nm. In order to estimate the second characteristic length, namely the penetration depth $\lambda(0)$, we use the

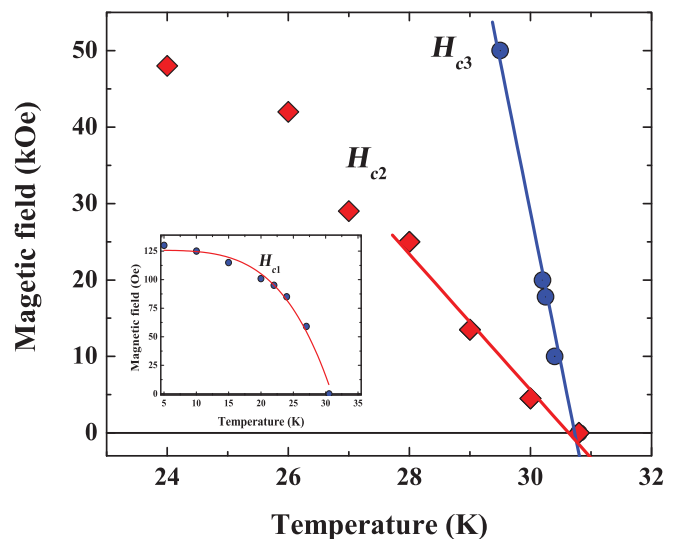


FIG. 3. (Color online) H - T phase diagram. Inset: Temperature dependence of H_{c1} . All lines are to guide the eye.

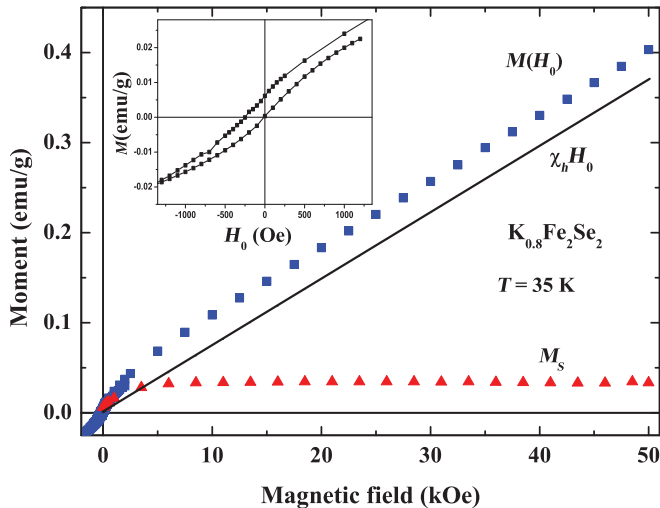


FIG. 4. (Color online) Magnetization curves in a normal state, $T = 35$ K. The inset shows the shifted hysteresis loop obtained at low H_0 . See text.

useful relationship $2H_{c1}(0)/H_{c2}(0) = [\ln(\kappa) + 0.5]/\kappa^2$, where $\kappa = \lambda(0)/\xi(0)$ is the GL parameter. Solving this equation numerically, we obtained $\kappa \approx 58$, from which $\lambda(0) \approx 580$ nm is deduced.

From the experimental hysteresis loop width, the critical current density (J_c) can be estimated by using the Bean critical state model, $J_c = 20\Delta M/a(1 - a/3b)$, where ΔM is the magnetization loop width at a given H_0 , and a and b are the crystal dimensions perpendicular to H_0 , where $a < b$. At 5 K for $H_0 = 10$ kOe, the estimated J_c is $\approx 10^3$ A/cm², a value that does not change much with field (up to 50 kOe) and agrees well with Ref. 18. We are aware of the fact that, for this orientation, an additional term must be added to J_c as shown in Ref. 19. However, this crude estimated value shows that these materials cannot support large critical currents even at low temperatures. This J_c is much smaller than critical currents of the SC Fe-As based materials, such as $\text{Ba}_{1-x}\text{K}_x\text{Fe}_2\text{As}_2$ and $\text{Ba}(\text{Fe}_{1-x}\text{Co}_x)\text{As}_2$.²⁰

At 35 K (above T_c) at low H_0 , the $M(H_0)$ curve is not linear as expected for AFM materials (see Ref. 18) and may contain another minor ferromagnetic (FM) component as an extra phase not detectable by x-ray diffraction (Fig. 4). The slope of the linear part, which reflects the AFM nature of the sample, is ≈ 0.0021 emu/mole Oe, which corresponds to $\approx 0.77\mu_B/\text{Fe}$ (Fig. 4). This means that for $\vec{H}_0 \parallel \mathbf{ab}$, only a small fraction of the total Fe moment is affected by H_0 . At high H_0 , $M(H_0)$ is composed of a linear ($\chi_h \times H_0$) and a saturation M_S term. In accordance with the estimation, $\chi_h \approx 7.4 \times 10^{-6}$ emu/g \times Oe. Subtracting the linear part yields the saturation moment $M_S = 0.033$ emu/g, which is attributed to 0.015% of pure iron. Indeed, the presence of pure Fe was confirmed by our ⁵⁷Fe MS studies performed on the same crystal, to be published elsewhere. Irreversibility in $M(H_0)$ is observed at low H_0 , and the hysteresis loop obtained is shown in Fig. 4 (inset). This loop is not symmetric relative to the origin and is known as the exchange-bias (EB) phenomena.^{21,22} EB is associated with the exchange anisotropy created at the interface between AFM and FM materials. The main information deduced from this hysteresis loop is the magnetic coercive field $H_c = 130$ Oe

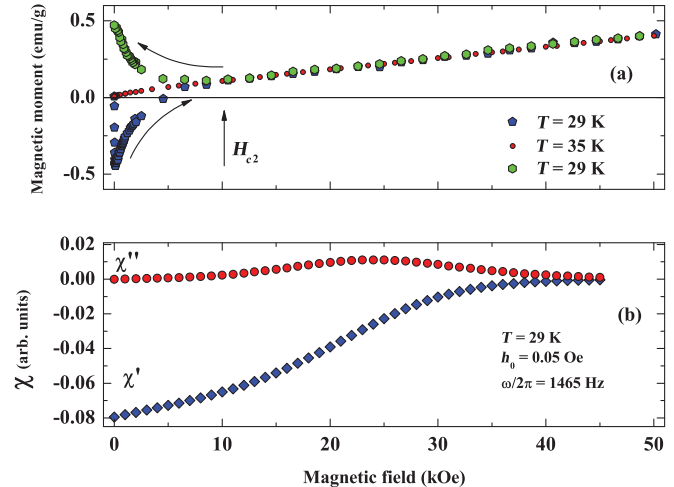


FIG. 5. (Color online) (a) Magnetization curve at $T = 29$ and 35 K. (b) Field dependencies of χ' and χ'' at $T = 29$ K.

and exchange bias $E_x = 65$ Oe, which is the loop shift from the origin. The discussion on EB is beyond the scope of the present paper. However, we may intuitively assume that this phenomenon is caused by the FM Fe particles immersed in the AFM matrix. This tiny amount of Fe affects the normal state only. As for the SC state, since $M(H_0)$ for Fe are linear at low H_0 up to ≈ 1 kOe and all $M(T)$ curves are practically constant at low temperatures, the deviation from linearity to determine $H_{c1}(T)$, as well as the onset of diamagnetic signals that determine H_{c2} , are not affected by the presence of 0.015% Fe.

The determination of the H_{c3} by resistivity and ac susceptibility methods has been well known since 1967; see Refs. 23 and 24. It is now well accepted that ac susceptibility studies are a powerful tool for determining the surface superconducting states, including determination of the surface critical field $H_{c3}(T)$; see Refs. 25 and 26 and references therein. A comparison between dc $M(H_0)$ and ac susceptibility measurements is depicted in Fig. 5. Figure 5(a) shows the ascending and descending $M(H_0)$ curves measured at 29 K and ascending $M(H_0)$ curve at 35 K from which H_{c2} can easily be

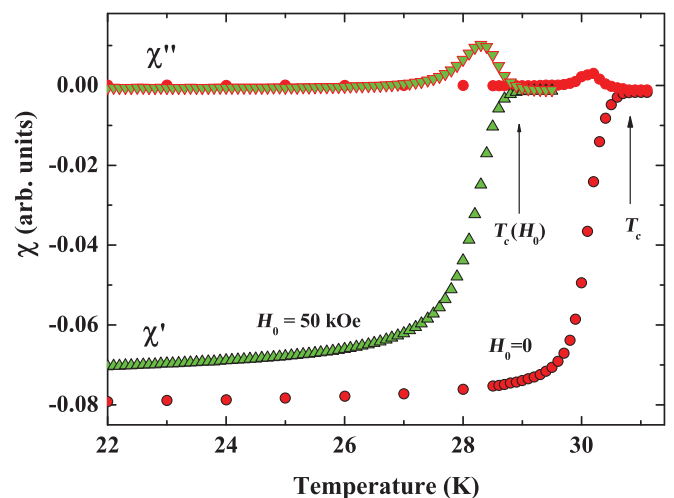


FIG. 6. (Color online) Temperature dependencies of χ' and χ'' at $H_0 = 0$ and 50 kOe.

determined (with the accuracy of ± 1 kOe), as discussed above. Note that the $H_0 > H_{c2}$ plot measured at 35 K coincides with the reversible data collected at 29 K. On the other hand, the real χ' and the imaginary χ'' ac susceptibility plots, measured under the same conditions, demonstrate clearly the existence of SC up to $H_{c3} > 50$ kOe, which is well above $H_{c2} \approx 13$ kOe. Two more examples of determining H_{c3} from $\chi'(T)$ and $\chi''(T)$ measured at $H_0 = 0$ and 50 kOe are presented in Fig. 6. Here we can obtain $T_c(H_0)$ with an accuracy of about ± 0.5 K. From the obtained data, $H_{c3}(T)$ was deduced and shown in Fig. 3. Note that, at $H_0 = 0$, the value obtained is T_c . The slope of the $H_{c3}(T)$ curve near T_c is ≈ -40 kOe/K. Therefore, the H_{c3}/H_{c2} ratio is ≈ 4.4 , a value which is much larger than the 1.7 predicted for single band conventional superconductors.

In several publications, $H_{c2}(T)$ was deduced from resistivity and/or ac susceptibility measurements. Indeed, these studies provide accurate $H_{c2}(T)$ values when the dc field is applied perpendicular to the **ab** crystal plane. In this geometry, the nucleation of the SC state starts at $H_0 < H_{c2}$.¹¹ On the other hand, for \vec{H}_0 parallel to the **ab** plane, this nucleation starts at H_{c3} , which is always higher than H_{c2} .^{11,25,26} For this geometry, $H_{c2}(T)$ can be determined from bulk measurements, such as dc

$M(H_0)$ [see Fig. 5(a)] and/or specific heat capacitance studies. Therefore, the high $H_{c2}(T)$ values reported for \vec{H}_0 parallel to the **ab** plane in Refs. 7 and 8 and in several other publications are presumably the surface $H_{c3}(T)$ plots. This issue needs more consideration.

In summary, we have performed dc and ac magnetization measurements from which all three critical fields for the SC $K_{0.8}Fe_2Se_2$ single crystal are determined. Evaluating $H_{c1}(0) \approx 130$ Oe and $H_{c2}(0) \approx 193$ kOe permits us to calculate the coherence length $\xi(0) \approx 10$ nm and the penetration depth $\lambda(0) \approx 580$ nm. Our ac susceptibility study provides for the first time the determination of $H_{c3}(T)$ for \vec{H}_0 parallel to the **ab** plane. The high $H_{c3}/H_{c2} \approx 4.4$ obtained needs more consideration.

The research in Jerusalem is partially supported by the Israel Science Foundation (ISF, Bikura 459/09), by the joint German-Israeli DIP project, and by the Klachky Foundation for Superconductivity. The authors are deeply grateful to V. M. Genkin and M. A. Belogolovskii for valuable discussions.

¹I. Felner, I. Mayer, A. Grill, and M. Schieber, *Solid State Commun.* **16**, 1005 (1975).

²H. Pinto and H. Shaked, *Phys. Rev. B* **7**, 3261 (1973).

³Q. Huang, Y. Qiu, W. Bao, M. A. Green, J. W. Lynn, Y. C. Gasparovic, T. Wu, G. Wu, and X. H. Chen, *Phys. Rev. Lett.* **101**, 257003 (2008).

⁴W. Bao, Q. Huang, G. F. Chen, M. A. Green, D. M. Wang, J. B. He, X. Q. Wang, and Y. Qiu, *Chin. Phys. Lett.* **28**, 086104 (2011).

⁵N. Ni, A. Thaler, J. Q. Yan, A. Kracher, E. Colombier, S. L. Bud'ko, P. C. Canfield, and S. T. Hannahs, *Phys. Rev. B* **82**, 024519 (2010).

⁶A. P. Dioguardi, N. apRoberts-Warren, A. C. Shockley, S. L. Bud'ko, N. Ni, P. C. Canfield, and N. J. Curro, *Phys. Rev. B* **82**, 140411(R) (2010).

⁷R. H. Liu, X. G. Luo, M. Zhang, A. F. Wang, J. J. Ying, X. F. Wang, Y. J. Yan, Z. J. Xiang, P. Cheng, G. J. Ye, Z. Y. Li, and X. H. Chen, *Europhys. Lett.* **94**, 27008 (2011); e-print arXiv:1104.4941.

⁸E. D. Mun, M. M. Altarawneh, C. H. Mielke, V. S. Zapf, R. Hu, S. L. Bud'ko, and P. C. Canfield, *Phys. Rev. B* **83**, 100514 (2011).

⁹Y. Mizuguchi, H. Takeya, Y. Kawasaki, T. Ozaki, S. Tsuda, T. Yamaguchi, and Y. Takano, *Appl. Phys. Lett.* **98**, 042511 (2011).

¹⁰H. D. Wang, C. H. Dong, Z. J. Li, Q. H. Mao, S. S. Zhu, C. H. Feng, H. Q. Yuan, and M. H. Fang, *Europhys. Lett.* **93**, 47004 (2011).

¹¹P. G. de Gennes, *Superconductivity of Metals and Alloys* (W. A. Benjamin, New York, 1966), p. 197.

¹²J. Guo, S. Jin, G. Wang, S. Wang, K. Zhu, T. Zhou, M. He, and X. Chen, *Phys. Rev. B* **82**, 180520(R) (2010).

¹³Y. J. Yan, M. Zhang, A. F. Wang, J. J. Ying, Z. Y. Li, W. Qin, X. G. Luo, J. Q. Li, J. Hu, and X. H. Chen, e-print arXiv:1104.4941.

¹⁴G. I. Leviev, V. M. Genkin, M. I. Tsindlekht, I. Felner, Yu. B. Paderno, and V. B. Filippov, *Phys. Rev. B* **71**, 064506 (2005).

¹⁵C. Ren, Z. S. Wang, H. Q. Luo, H. Yang, L. Shan, and H. H. Wen, *Physica C* **469**, 599 (2009).

¹⁶N. R. Werthamer, E. Helfand, and P. C. Hohenberg, *Phys. Rev.* **147**, 295 (1966).

¹⁷Y. Zhang, L. X. Yang, M. Xu, Z. R. Ye, F. Chen, C. He, H. C. Xu, J. Jiang, B. P. Xie, J. J. Ying, X. F. Wang, X. H. Chen, J. P. Hu, M. Matsunami, S. Kimura, and D. L. Feng, *Nat. Mater.* **10**, 273 (2011).

¹⁸R. Hu, K. Cho, H. Hodovanets, W. E. Straszheim, M. A. Tanatar, R. Prozorov, S. L. Bud'ko, and P. C. Canfield, e-print arXiv:1102.1931.

¹⁹M. A. Tanatar, N. Ni, C. Martin, R. T. Gordon, H. Kim, V. G. Kogan, G. D. Samolyuk, S. L. Bud'ko, P. C. Canfield, and R. Prozorov, *Phys. Rev. B* **79**, 094507 (2009).

²⁰B. Shen, P. Cheng, Z. Wang, L. Fang, C. Ren, L. Shan, and H.-H. Wen, *Phys. Rev. B* **81**, 014503 (2010); e-print arXiv:1104.4950.

²¹J. Nogues and I. K. Schuller, *J. Magn. Magn. Mater.* **192**, 203 (1999).

²²M. R. Fitzsimmons, P. Yashar, C. Leighton, I. K. Schuller, J. Nogués, C. F. Majkrzak, and J. A. Dura, *Phys. Rev. Lett.* **84**, 3986 (2000).

²³H. R. Hart Jr. and P. S. Swartz, *Phys. Rev.* **156**, 403 (1967).

²⁴R. W. Rollins and J. Silcox, *Phys. Rev.* **155**, 404 (1967).

²⁵M. I. Tsindlekht, V. M. Genkin, G. I. Leviev, I. Felner, O. Yuli, I. Asulin, O. Millo, M. A. Belogolovskii, and N. Yu. Shitsevalova, *Phys. Rev. B* **78**, 024522 (2008).

²⁶J. Kötzler, L. von Sawilski, and S. Casalbuoni, *Phys. Rev. Lett.* **92**, 067005 (2004).